Identification and validation of a novel prognostic model based on anoikis-related genes in acute myeloid leukemia

YUNDONG CHEN[1,2], WENCONG LUO[1,2], MINGYUE HU[3], XIAOYU YAO[1,2], JISHI WANG[1] and YI HUANG[1]

[1]Department of Hematopathology, The Affiliated Hospital of Guizhou Medical University, Guiyang, Guizhou 550004, P.R. China;
[2]Department of Clinical Medicine, Guizhou Medical University, Guiyang, Guizhou 550025, P.R. China;
[3]College of Computer Science and Technology, Guizhou University, Guiyang, Guizhou 550025, P.R. China

Abstract. Acute myeloid leukemia (AML) is a hematological cancer prevalent worldwide. Anoikis-related genes (ARGs) are crucial in the progression of cancer and metastasis of tumors. However, their role in AML needs to be clarified. In the present study, differential analysis was performed on data from The Cancer Genome Atlas database to identify differentially expressed ARGs (DE-ARGs). Subsequently, a prognostic model for patients with AML was constructed using univariate Cox, Least Absolute Shrinkage and Selection Operator and multivariate Cox regression analyses. This model was based on four key DE-ARGs [lectin galactoside-binding soluble 1 (LGALS1), integrin subunit α 4 (ITGA4), hepatocyte growth factor (HGF) and Ras homolog gene family member C (RHOC)]. Independent prognostic factors for AML included prior treatment, age, risk scores and diagnosis. A nomogram was constructed based on these factors to aid clinical decision-making. Furthermore, bone marrow samples were collected from individuals diagnosed with AML and healthy donors to validate the expression of the identified ARGs using reverse transcription-quantitative PCR. The mRNA levels of LGALS1 and RHOC were significantly higher, while those of ITGA4 and HGF were significantly lower in patients with AML than in healthy donors (all P<0.05). The results of the present study expands the understanding of the function of ARGs in AML, providing a new theoretical basis for the treatment of AML.

Correspondence to: Professor Yi Huang or Professor Jishi Wang, Department of Hematopathology, The Affiliated Hospital of Guizhou Medical University, 9 Beijing Road, Guiyang, Guizhou 550004, P.R. China
E-mail: 932034291@qq.com
E-mail: wangjishi9646@163.com

Introduction

Acute myeloid leukemia (AML) is a blood cancer characterized by the abnormal growth and accumulation of cells in the hematopoietic system (1). It is the most common type of AML in adults, with ~20,380 new cases and 11,310 deaths in 2023 (2). Despite extensive research on prognostic biomarkers, the prognosis of AML remains highly variable, with a <50% 5-year overall survival (OS) rate and only a 20% survival rate for elderly patients 2 years post-diagnosis (3). Currently, cytogenetic and molecular abnormalities at diagnosis are considered the most important prognostic factors, predicting complete remission rates, disease-free survival, relapse risk and OS.

Anoikis, a form of programmed cell death, occurs when cell-cell or cell-extracellular matrix attachments are disrupted, contributing to tissue homeostasis maintenance by eliminating misplaced or dislodged cells (4). Cancer cells often evade anoikis through several mechanisms, resulting in enhanced invasiveness and metastatic potential (5). Anoikis-related genes (ARGs) are crucial in driving the overall progression and metastatic cascade across several cancers, such as gastric carcinoma (6), lung cancer (7), breast carcinoma (8) and endometrial carcinoma (9).

Patients with AML and elevated lectin galactoside-binding soluble 1 (LGALS1) mRNA levels exhibit reduced disease-free survival (10). Additionally, hepatocyte growth factor (HGF) affects leukemic cell proliferation and migration (11), whilst integrin subunit α 4 (ITGA4) mediates anti-apoptotic signals, conferring chemoresistance (12). Both *in vivo* and *in vitro* studies have demonstrated the critical role of Ras homolog gene family member C (RhoC) in promoting metastasis by protecting metastatic cells from apoptosis, influencing cell motility and modulating chemokine secretion (13). Despite its substantial impact on tumorigenesis and metastasis, the role of anoikis in AML remains unclear.

The present study aimed to identify hub genes associated with anoikis in patients with AML and enhance the predictive power of highly influential genes through several analyses, including univariate and multivariate Cox regressions, differential expression analysis and Least Absolute Shrinkage and Selection Operator (LASSO) regression. Using these identified ARGs, the present study performed prognostic assessments,

functional enrichment analysis and principal component analysis (PCA) in patients with AML. Ultimately, a risk signature was developed to assess the predictive value of ARGs in AML, aiming to provide a novel prognostic tool for patients with this pathology.

Materials and methods

Data acquisition of patients with AML. The survival data and RNA-sequencing (RNA-seq) data of 151 patients with AML were obtained from The Cancer Genome Atlas (TCGA) using the publicly available University of California, Santa Cruz Xena database (https://xenabrowser.net/datapages/). A training set comprising 132 patients with AML with comprehensive clinical information and survival data was used for subsequent analysis. The GSE71014 dataset, containing RNA-seq and survival data from 104 patients with AML, was sourced from the Gene Expression Omnibus (GEO) database (https://www.ncbi.nlm.nih.gov/geo/) and served as the validation set. In a previous study, 434 ARGs were identified (14).

Identification of anoikis-related subtypes in the training set. The R package 'ConsensusClusterPlus' version 1.54.0 (15) was used to identify subtypes associated with anoikis, based on the expression of the 434 ARGs. The clustering results were validated using PCA. The OS among different subtypes was further assessed using the 'Survival' package version 3.2-3.

Simultaneously, the 'limma' package version 3.52.4 (16) was used for differential expression analysis to identify differentially expressed ARGs (DE-ARGs) between the two identified subtypes. The screening criteria were set as P<0.05 and |log$_2$FoldChange|>0.5. The 'clusterProfiler' version 4.4.4 (15) was used to perform Gene Ontology (GO) and Kyoto Encyclopedia of Genes and Genomes (KEGG) enrichment analyses on these DE-ARGs. The results were visualized using bubble plots with the R package 'ggplot2' version 3.3.2 (The R Foundation) (17).

Construction and validation of the prognostic risk model. A univariate Cox analysis of DE-ARGs was performed in the training set to identify the prognosis-related genes (P<0.05). The most predictive prognostic genes were identified through using LASSO (18) and multivariate Cox analyses. Subsequently, patients in the training set were stratified into two groups based on the median risk score. The differences in OS between the two groups were visualized using Kaplan-Meier (KM) curves using the 'survminer' package 3.6.0 (19). To assess the prognostic capability of the model, receiver operating characteristic (ROC) curves were developed using the 'survival ROC' package 1.42.0 (20). Finally, the prognostic model was validated using the external validation dataset GSE71014.

Analysis of independent prognostic factors. Univariate and multifactorial Cox analyses were performed to determine the association between clinicopathological characteristics and risk scores, and identify independent predictive factors for AML. The 'rms' package version 6.0-1 (21) was used to develop a nomogram predicting survival probability based on independent prognostic criteria. Calibration curve and decision curve analyses were used to validate the suitability of the nomogram for clinical decision-making.

Biological differences between the two groups. The limma package version 3.52.4 (16) was used to identify differentially expressed genes (DEGs), with criteria set at |log$_2$FC|>0.5 and adjusted P-value (P.adjust) <0.05. Subsequently, a functional enrichment analysis on these DEGs was performed using the R package 'clusterProfiler' version 4.4.4 (The R Foundation).

Distribution of clinicopathological features for risk score determination. In the training set, clinical information was extracted, such as cytogenetic risk categories mentioned in the published literature (intermediate/normal, favorable, unknown or poor) (22), sex (female or male), prior treatment and diagnosis (No or Yes) and age (>60 or ≤60 years) of patients with AML. The phenotype data of the TCGA AML dataset were downloaded from the Xena database (https://gdc-hub.s3.us-east-1.amazonaws.com/download/TCGA-LAML.GDC_phenotype.tsv.gz) to extract clinical features including cytogenetics risk category, sex, 'prior_treatment.diagnoses' and age. The cytogenetics risk category was categorized into intermediate/normal, favorable, poor and unknown groups according to the cytogenetics risk category column in the downloaded phenotype file. Differences in risk scores between subgroups with different clinical characteristics were subsequently compared using Wilcoxon rank-sum tests (comparison between two groups) and the Kruskal-Wallis test (comparison between multiple groups) to determine significant differences between clinical conditions (P<0.05. Dunn's test was used as the post hoc test. The 'ComplexHeatmap' version 1.14.0 (23) was used to visualize the results.

Reverse transcription (RT)-quantitative (q)PCR analyses. Bone marrow samples were collected from 20 individuals diagnosed with AML, including newly diagnosed patients and those who had relapsed. The control group consisted of healthy donors matched for age and sex with the patients. Allogeneic hematopoietic stem cell donors were recruited from patients scheduled for hematopoietic stem cell transplantation at Guizhou Medical University (Guiyang, China) between February 2022 and October 2023. Ethical approval for the present study was obtained from The Ethics Committee of the Affiliated Hospital of Guizhou Medical University (approval no. 2023-744). The donors were all family members or friends of patients who were then hospitalized. Prior to the donation, all patients underwent bone marrow aspiration to assess the normality of bone marrow morphology according to hospital requirements. The present study was performed in accordance with the principles of the Declaration of Helsinki, and all patients provided written informed consent prior to enrollment. Table SI presents information on the patients with AML.

RNA extraction was performed using an Ultra Pure RNA Extraction kit (cat. no. CW0581; Jiangsu CoWin Biotech Co, Ltd.), followed by RT at 55˚C for 5 min to generate cDNA using a Reverse Transcription cDNA kit (cat. no. K1622; Thermo Fisher Scientific, Inc.). qPCR was performed with SYBR Green Master Mix (cat. no. NVZ-Q221-01; Vazyme Biotech Co., Ltd.), using an Applied Biosystems 7500 Real-Time Cycler (QuantStudio 1; Applied Biosystems; Thermo Fisher
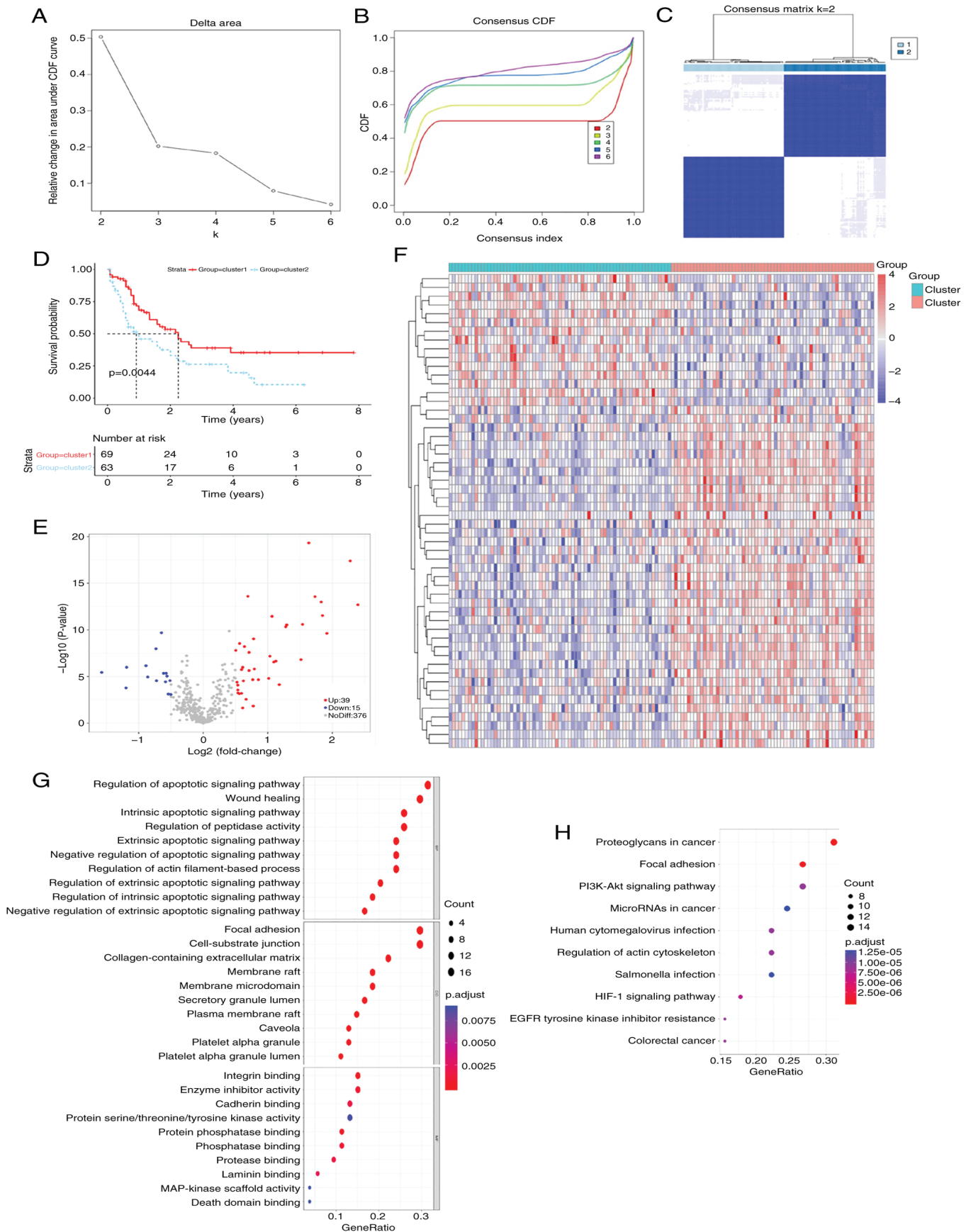
Figure 1. Differential analysis between anoikis-related subtypes and enrichment analysis. (A) Cluster analysis performed using The Cancer Genome Atlas-Acute myeloid leukemia cohort (n=132) using the expression matrix of ARGs showing the changes in values and (B) the downward trend of CDF. (C) Cluster effect diagram of two subtypes of samples. (D) Kaplan-Meier analysis of patient outcomes between different clusters. (E) Volcano map of the differential expression of the 54 ARGs between cluster 1 and 2. (F) Heatmap demonstrating expression patterns of the 54 ARGs. (G) Bubble plot of Gene Ontology top 10 enrichment results for 54 ARGs. (H) Bubble plot of Kyoto Encyclopedia of Genes and Genomes top 10 enrichment results for 54 ARGs. CDF, cumulative distribution function; ARGs, anoikis-related genes.
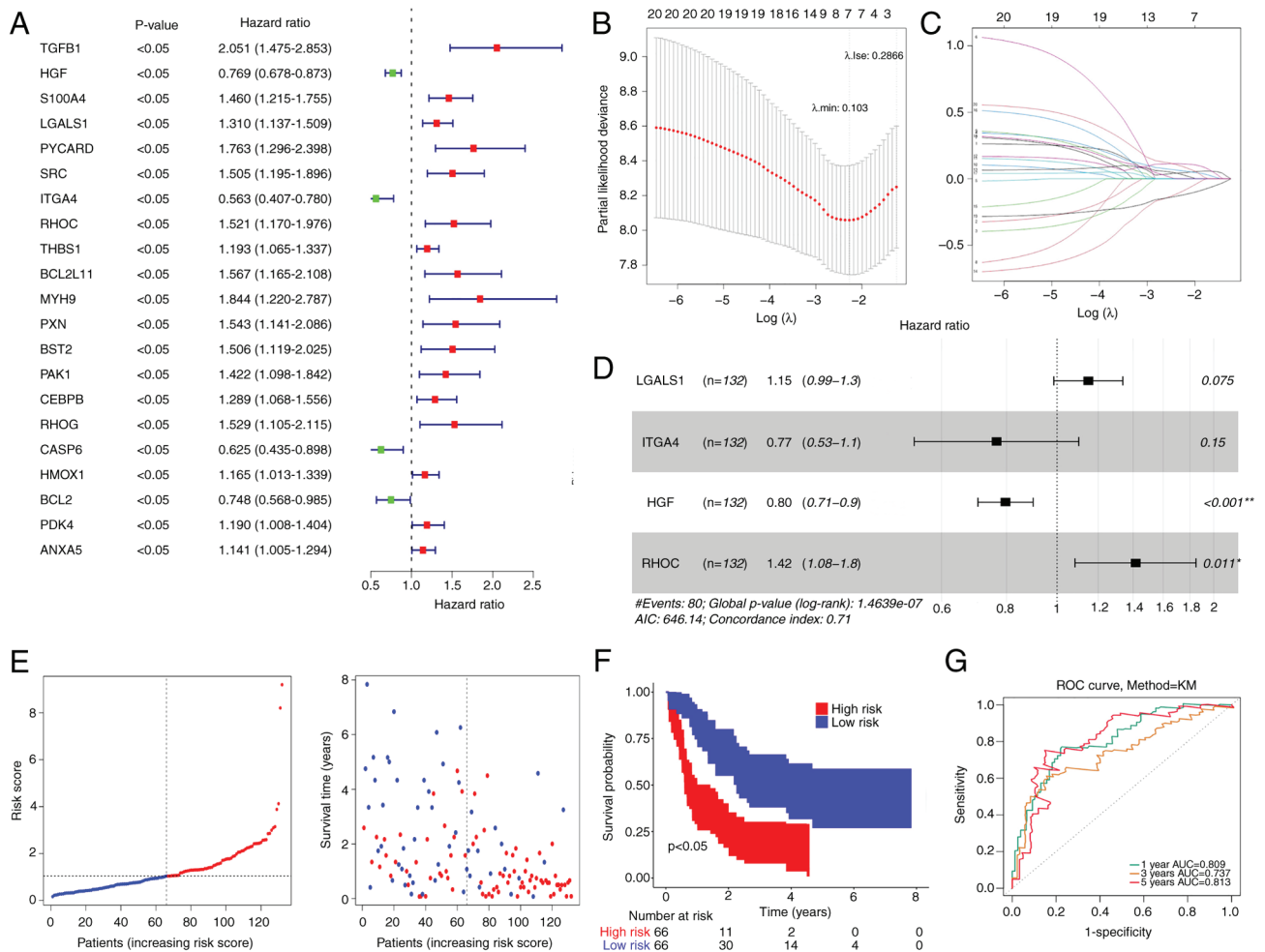
Figure 2. Prognostic risk model development and validation. (A) Univariate Cox analysis of DE-ARGs. (B) Abscissa represents log (λ) and the ordinate denotes the error of cross-validation. (C) Each curve represents the change trajectory for each independent variable coefficient. (D) Multifactorial Cox analysis of DE-ARGs that passed least absolute shrinkage and selection operator regression analysis. (E) Distribution of patients into high- and low-risk groups in the training set. (F) KM survival analysis of patients in the high- and low-risk groups. (G) ROC curves of patients at 1, 3 and 5 years. DE-ARGs, differentially expressed anoikis-related genes, ROC, receiver operating characteristic, KM, Kaplan-Meier, AUC, area under the curve; LGALS1, lectin galactoside-binding soluble 1; ITGA4, integrin subunit α4; HGF, hepatocyte growth factor; RHOC, Ras homolog gene family member C.

Scientific, Inc.). PCR conditions included an initial denaturation step at 95˚C for 10 min, followed by 40 cycles of denaturation at 95˚C for 15 sec, and annealing/extension at 60˚C for 1 min, with a standard melting curve analysis performed afterward. All samples were analyzed in triplicate, and gene expression levels were quantified using the comparative threshold cycle method ($2^{-\Delta\Delta Cq}$) with GAPDH serving as the reference gene for normalization (24). Primer pairs and corresponding sequences used in the present study are detailed in Table SII.

Prediction of chemotherapy drug. The oncoPredict tool version 0.2 (25) was used to predict chemotherapy agents for AML using data from the Genomics of Drug Sensitivity in Cancer (GDSC) database (https://www.cancerrxgene.org/). The half-maximal inhibitory concentration (IC_{50}) values were calculated for each patient with AML in the two groups. To compare differences in drug sensitivity between the two groups, the Wilcoxon rank-sum test was used.

Statistical analysis. R software (version 4.2.2; The R Foundation) was used for all analyses. The Wilcoxon rank-sum

test was used to compare data between the two groups. The Kruskal-Wallis test was used for multiple comparisons, followed by Dunn's post hoc test. $P < 0.05$ was considered to indicate a statistically significant difference.

Results

Identification of anoikis-related subtypes. Using the expression profiles of ARGs, 132 AML samples were classified through the consensus clustering analysis method. The consistency distribution for k values ranging from 2-6 was displayed in an empirical cumulative distribution function plot. The consensus matrix heatmap revealed that k=2 was optimal for classification, dividing AML samples into cluster 1 and cluster 2 (Figs. 1A-C and S1; Table SIII). Patients in cluster 2 exhibited inferior prognoses compared with those in cluster 1 (Fig. 1D), indicating that AML prognosis is influenced by ARG expression levels and supporting the subsequent screening of survival-related ARGs. A difference in the expression of 54 ARGs was observed between the two subtypes (Fig. 1E and F). Using a significance threshold of
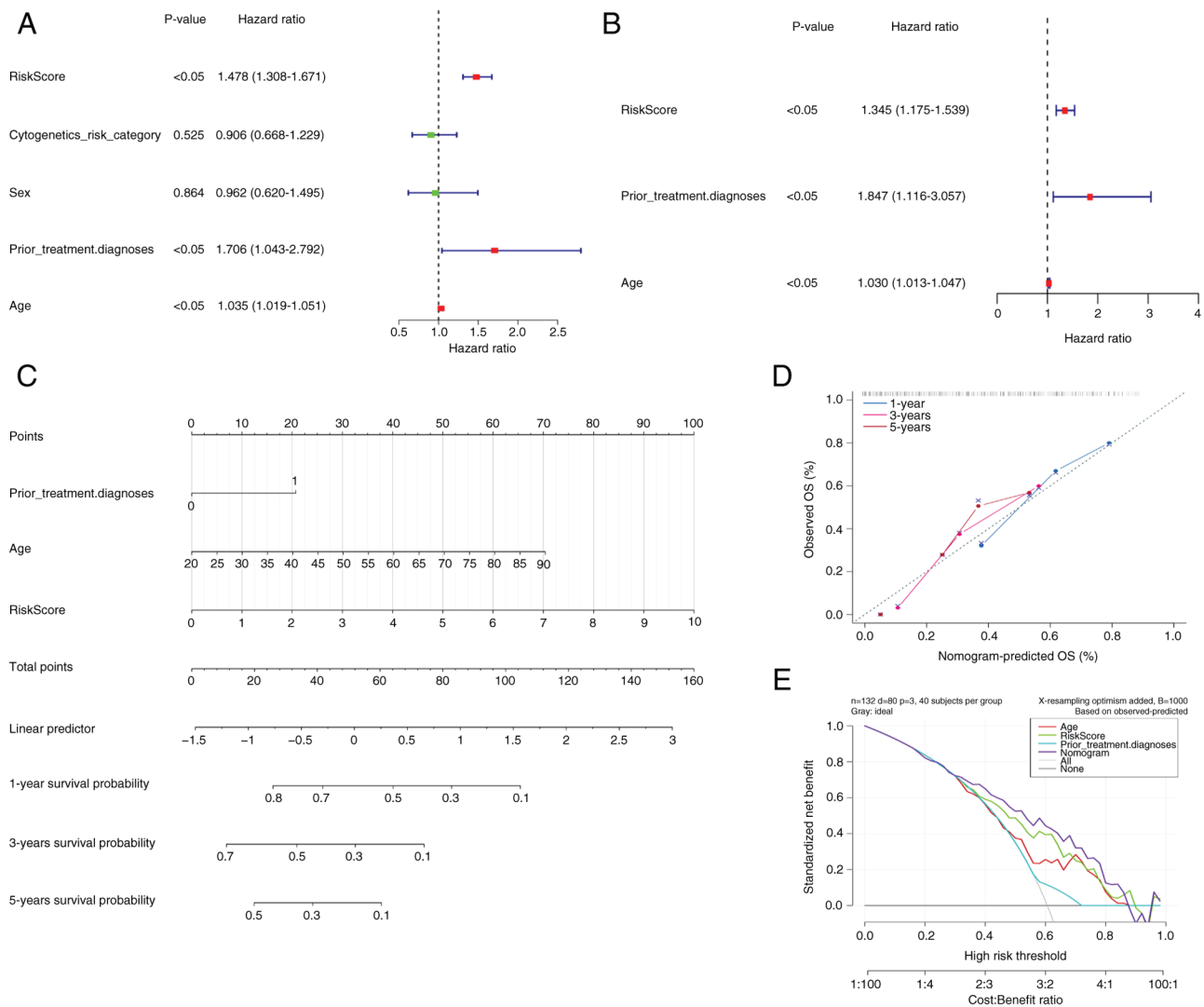
Figure 3. Development and assessment of the nomogram model. Forest plots demonstrating (A) univariate and (B) multivariate Cox independent prognostic analysis of clinical characteristics and risk scores (C) Nomogram constructed based on independent prognostic factors. (D) Calibration curve evaluating the predictive power of the nomogram model. (E) Clinical benefits of the nomogram model surpassed those of the age curve, riskScore curve, prior treatment and diagnoses curve within the risk threshold range of 0-1. OS, overall survival.

P.adjust <0.05, 1,067 GO terms and 104 KEGG pathways were associated with these DEGs (Fig. 1G and H). GO analysis revealed that these DEGs were involved in the regulation of the intrinsic apoptotic signaling pathway, regulation of peptidase activity, apoptotic signaling pathway, focal adhesion and cell-substrate junction. Additionally, DEGs were significantly associated with microRNA (miR) in cancer, phosphatidylinositol 3-kinase (PI3K)/protein kinase B (Akt) signaling pathway and proteoglycans in cancer.

Development of an effective prognostic risk model associated with anoikis in AML. Using DE-ARGs, 21 genes with P<0.05 were identified in the training set (Fig. 2A). Subsequently, LASSO regression analysis was performed to exclude false positive genes (Fig. 2B and C). Finally, four prognostic ARGs were determined using multifactorial Cox analysis: LGALS1, ITGA4, HGF and RHOC (Fig. 2D).

The risk score was calculated as follows: Risk score = 0.13836534 x LGALS1-0.26749323 x ITGA4-0.227481177 x HGF + 0.3471619 x RHOC.

Patients were stratified into two groups based on a median risk of 1.042299 (Fig. 2E). Patients with low-risk scores demonstrated significantly higher OS rates compared with those with high-risk scores (Fig. 2F). The validity of the risk signature was further assessed by computing the ROC curve for OS. The area under the curve (AUC) values were >0.70 at 1, 3 and 5 years, indicating enhanced efficacy of the prognostic risk model (Fig. 2G).

The model was validated using the GSE71014 dataset, and AML samples were stratified based on the median risk score. As the risk score increased, the OS of patients with AML gradually decreased, accompanied by a steady rise in mortality rates (Fig. S2A and B). KM curves in the GSE71014 dataset revealed that patients with AML in the low-risk group had significantly longer OS rates compared with those in the high-risk group (P<0.05; Fig. S2C). Furthermore, the AUC values for 1-, 3- and 5-year survival rates based on this model were 0.809, 0.737 and 0.813, respectively, indicating enhanced efficacy of the prognostic risk model (Fig. S2D).
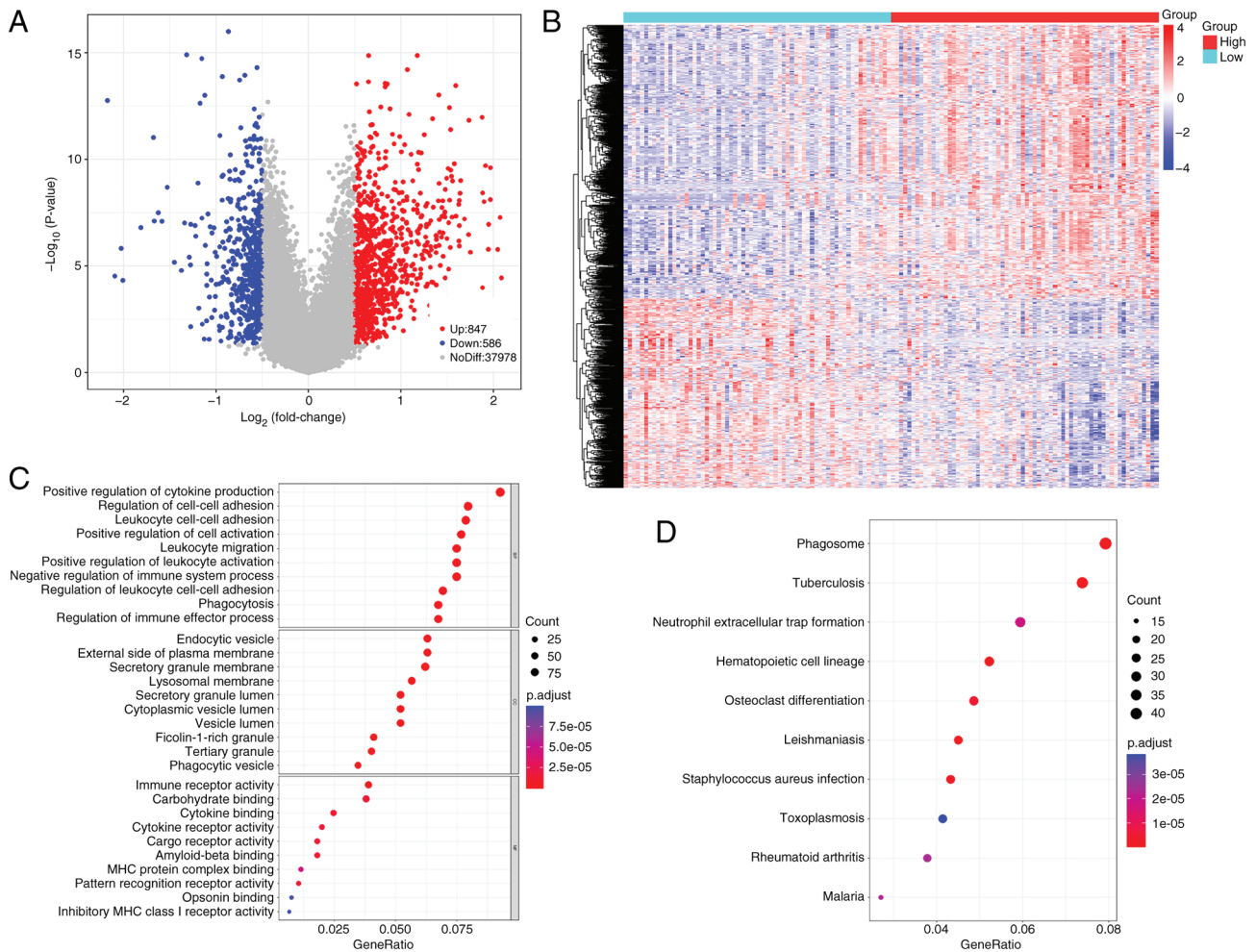
Figure 4. Identification of DEGs and their enrichment analysis. (A) Volcano map and (B) heatmap demonstrating the DEGs. In the heatmap, the first row represents sample grouping, with each subsequent row representing the expression level of individual genes across different samples, and each column indicating the expression level of all differentially expressed genes within each sample. The tree on the left side illustrates the results of cluster analysis, grouping different genes from several samples. Top 10 enriched pathways associated with DEGs using (C) Gene Ontology and (D) Kyoto Encyclopedia of Genes and Genomes analyses. DEGs, differentially expressed genes.

Construction of a nomogram model with accurate prediction. The clinicopathological variables and risk scores from 132 patients were combined to perform univariate and multivariate Cox regression analyses (Fig. 3A and B). Risk scores, prior treatment, diagnosis and age were demonstrated to be independent prognostic factors for patients with AML. Based on these factors, a nomogram model was constructed (Fig. 3C), indicating a marked decrease in survival rate with an increasing overall score. The calibration curve yielded a c-index of 0.942 for this nomogram model, demonstrating its high predictive accuracy and reliability (Fig. 3D). Therefore, the nomogram emerged as the optimal model (Fig. 3E).

Identification of DEGs and their functional enrichment analysis. A total of 1,433 DEGs between the two groups were identified (Table SIV). Volcano and heatmap representations of these DEGs are presented in Fig. 4A and B. Screening based on P.adjust values <0.05 yielded 1,218 GO terms and 59 KEGG pathways (Fig. 4C and D). These DEGs were significantly associated with regulation of cell-cell adhesion, positive regulation of cytokine production, endocytic vesicles and leukocyte cell-cell adhesion. DEGs were significantly involved in

phagosome formation, neutrophil extracellular trap formation, hematopoietic cell lineage and osteoclast differentiation.

Association between risk scores, age and cytogenetics risk category. Significant differences in risk scores (P<0.05) were demonstrated across cytogenetics risk categories (favorable vs. intermediate/normal, favorable vs. poor and favorable vs. unknown) and age groups (Fig. 5A; Table SV). A total of four genes were notably associated with different clinical characteristics (Fig. 5B). Survival analysis stratified by clinical data revealed no significant differences in the cytogenetics risk category-favorable and prior treatment diagnosis-Yes subgroups, whilst significant differences were demonstrated in the remaining subgroups (Fig. 5C).

LGALS1, ITGA4, HGF and RHOC can be used as prognostic genes of AML. Multivariate Cox regression analysis revealed that LGALS1, RHOC, ITGA4 and HGF were notably associated with a favorable prognostic impact on patients with AML. As diagnostic biomarkers, the AUC of LGALS1, RHOC, ITGA4 and HGF were >0.6, indicating their high predictive accuracy in AML diagnosis (Fig. 6A).
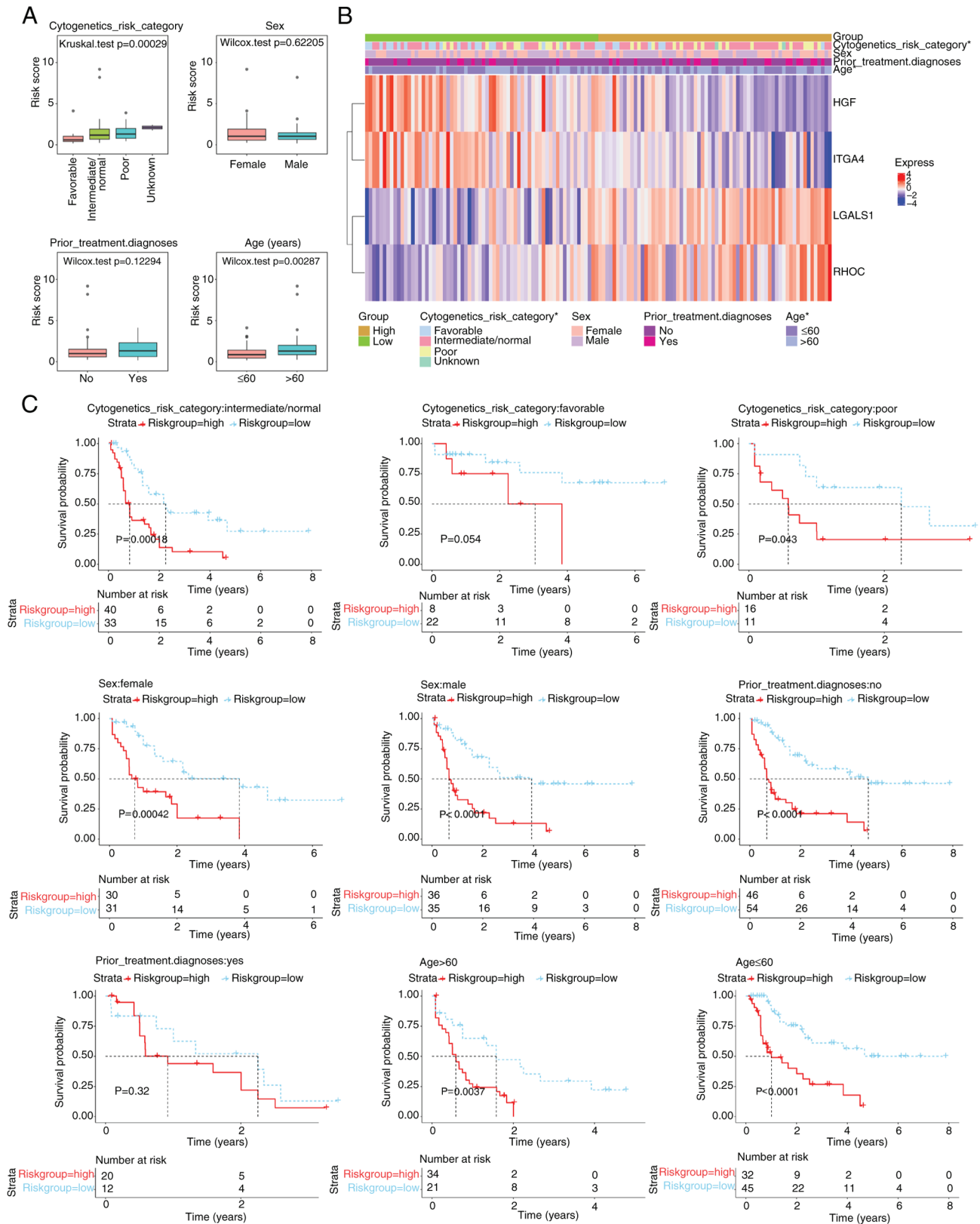
Figure 5. Association between risk scores and clinical characteristics. (A) Analysis of differences in risk scores among different clinical features. (B) Heatmap of biomarker expression differentially expressed between high- and low-risk groups and several clinical features. (C) Survival curves between groups with different clinical features.

Furthermore, LGALS1 and HGF expression levels were significantly lower, whilst ITGA4 and RHOC expression levels were significantly higher in patients with AML compared with the corresponding controls (all P<0.05; Fig. 6B). These results were further confirmed by RT-qPCR analysis (Fig. 6C). Additionally, mRNA expression levels of LGALS1 and RHOC were significantly higher, whilst those of ITGA4 and HGF were significantly lower in patients with
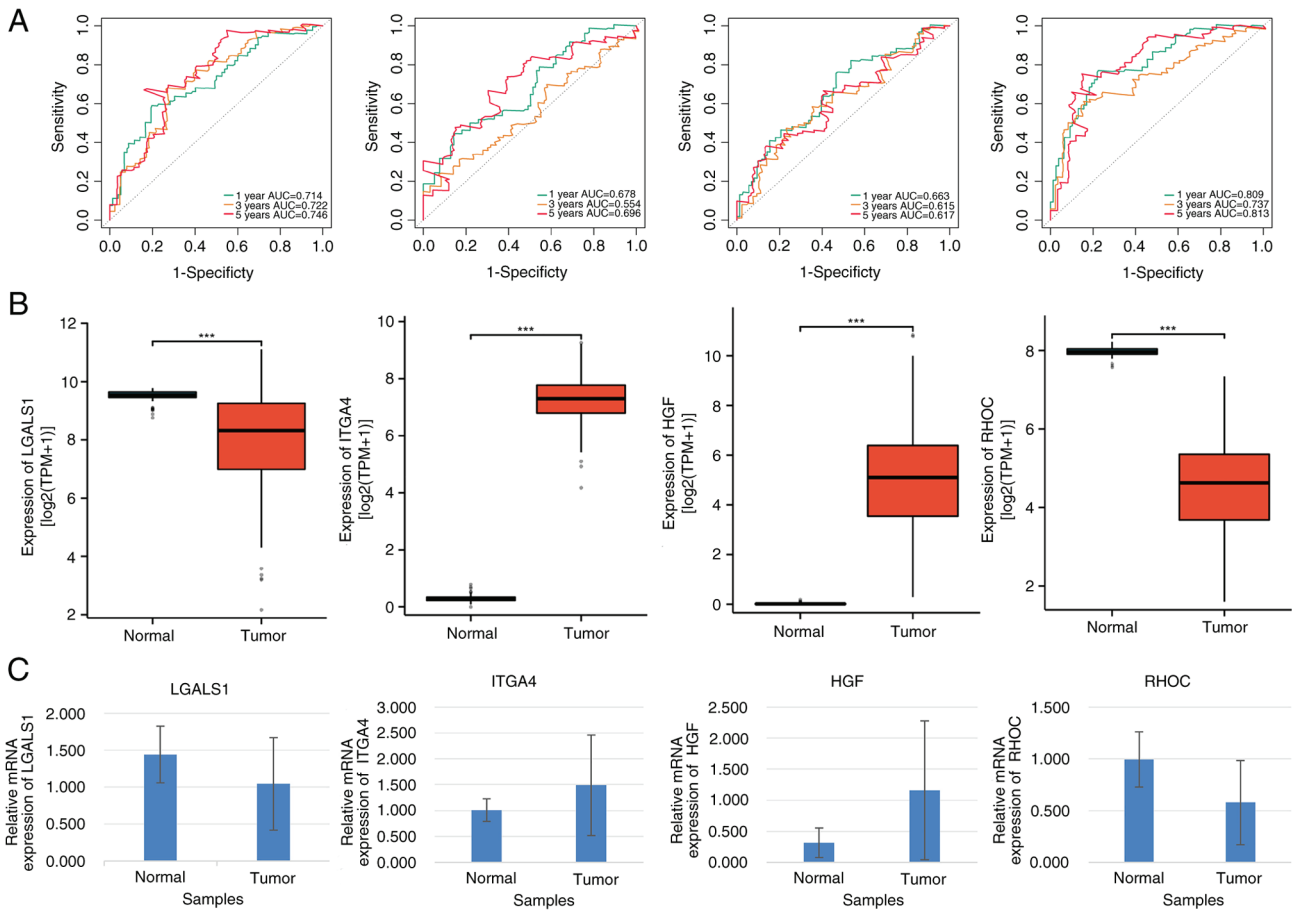
Figure 6. Prognostic and clinical value analyses of LGALS1, ITGA4, HGF and RHOC in patients with AML. (A) Receiver operating characteristic curves of LGALS1, ITGA4, HGF and RHOC. (B) Gene expression levels of LGALS1, ITGA4, HGF and RHOC in AML and normal control samples. (C) Reverse transcription-quantitative PCR analysis of LGALS1, ITGA4, HGF and RHOC expression (P<0.05). ***P≤0.001. AML, acute myeloid leukemia, AUC, area under the curve.

AML compared with their healthy counterparts (all P<0.05; Table SVI).

Sensitivity of AML-related drugs varies between high- and low-risk groups. The IC_{50} values were calculated for each patient with AML in the two groups. In total, 138 drugs demonstrated significant IC_{50} values (Table SVII). Box plots in Fig. 7 demonstrate the IC_{50} values for the top 10 significantly different treatment-sensitive drugs. These results indicate substantial disparity between the high- and low-risk groups, with the former exhibiting considerably higher IC_{50} values.

Discussion

AML is an aggressive form of cancer characterized by the rapid proliferation of immature myeloid leukemia cells (26). Whilst it primarily affects the bone marrow, malignant cells may also be found in the peripheral blood or other tissues (27,28). Despite advancements in therapeutic and diagnostic techniques, early diagnosis and treatment of AML remain challenging. Therefore, identifying new and highly accurate prognostic indicators for AML is an urgent and unmet need.

Anoikis, a form of programmed cell death, is crucial for tissue homeostasis and development by preventing the attachment or growth of dysplastic cells (29). Its dysregulation has been linked to cancer progression, promotion of tumor invasion and migration, and the development of drug resistance (30-32). However, limited research exists on the impact of ARGs on invasive mobility and drug resistance in AML, as well as their role in predicting AML prognosis.

The present study used the TCGA database and existing literature (14) to acquire relevant data and identify genes associated with the anoikis. Through consistent cluster, differential gene expression and functional enrichment analyses, four biomarker genes were identified (LGALS1, ITGA4, HGF and RHOC). Subsequently, a risk model was constructed using single-factor Cox, LASSO and stepwise multi-factor Cox regression analysis. The risk model was evaluated using the TCGA training set, stratifying it into high- and low-risk groups based on the median quantitative risk calculated from the four biomarkers. Moreover, the present study validated the effectiveness of the risk model through KM survival curves, ROC curves, risk curves and PCA. External validation using the GSE71014 dataset further confirmed the efficacy of the risk model. Prognostic analysis identified risk score, prior treatment, diagnosis and age as significant independent prognostic factors. Significant differences were also demonstrated in risk scores among cytogenetics risk categories and age groups. Finally, by evaluating TCGA training set with the GDSC

Figure 7. Analysis of acute myeloid leukemia-related drugs. Yellow boxes indicate low-risk groups, and blue boxes indicate high-risk groups. IC50, half-maximal inhibitory concentration.

database, 50 drugs with significant differences in efficacy between the high- and low-risk groups were identified.

The anoikis-related model (ARS model) proposed in the present study demonstrated a significant association with survival outcomes in AML cases. The ARS model comprises four ARGs: LGALS1, ITGA4, HGF and RHOC.

LGALS1, a member of the galectin family, is a protein with a strong affinity for β galactosides, regulating several tumor suppressors and promoters (33). LGALS1 is highly expressed in AML cells and is associated with a poor prognosis in affected patients. Furthermore, it promotes the survival and proliferation of AML cells by regulating the expression of apoptosis- and cell cycle-related proteins (10).

ITGA4 is a protein-coding gene belonging to the integrin α chain family. ITGA4 serves as a key molecule that allows AML cells to bind to bone marrow stromal elements and facilitates cellular migration. Methyltransferase-like 3 has been reported to increase the stability of ITGA4 mRNA transcripts through N6-methyladenosine modification, leading to its upregulation on the cell surface and promoting AML cell homing and engraftment (34).

The HGF gene, located on the long arm of chromosome 7 (7q2111), encodes a precursor protein consisting of 728 amino acids. Under normal conditions, the HGF/mesenchymal-epithelial transition factor (c-MET) signaling pathway serves a critical role in mediating interactions between epithelial and mesenchymal cells, which is essential for tissue repair, inflammation control and immune regulation (35). HGF upregulation emerged as a prominent compensatory mechanism, contributing to resistance against MET inhibition in AML (36). A 29-fold higher expression of HGF was reported in bone marrow samples during refractory disease compared with remission. Additionally, HGF induces upregulation of matrix metalloproteinase (MMP)2 and MMP9 expression, facilitates cell cycle progression, suppresses apoptosis and enhances cell proliferation through activation of the PI3K/AKT and mitogen-activated protein kinase (MAPK)/extracellular signal-regulated kinase (ERK) signaling pathways (37). Collectively, these investigations highlight the pivotal role of the HGF/c-MET signaling pathway in AML.

RhoC, a member of the Rho family of small GTPases, regulates several cellular processes (38). Recent research assessed the involvement of the Rho subfamily in cellular migration (39). This subfamily includes highly homologous RhoA, RhoB and RhoC, which regulate actin cytoskeleton dynamics. Overexpression of miR-372 has been reported to lead to downregulation of RhoC expression via its 3' untranslated

region (3' UTR), thereby suppressing the proliferation, migration and invasion abilities of endometrial adenocarcinoma cells (40). Additionally, miR-10b has been reported to inhibit homeobox D10 in colorectal cancer, metastatic breast cancer and malignant glioma cells, upregulating RhoC expression (41,42). In ovarian cancer, miR-519d binds directly to the 3' UTR of RhoC mRNA, suppressing its expression, as reported in a nude mouse xeno-transplantation model (43). miR-493 directly regulates RhoC, leading to a marked decrease in its mRNA and protein expression levels, effectively suppressing the growth, invasion and metastasis of gastric cancer cells (44). Moreover, upregulation of RhoC expression has been reported to be notably associated with an unfavorable prognosis. Therefore, a strong negative association exists between RhoC expression and cancer prognosis, and these signature genes are closely associated with tumors.

Using the Gene set enrichment analysis algorithm, the present study identified several tumor signaling pathways activated in the high-risk group compared with that in the low-risk group. These included the PI3K/AKT and hypoxia-inducible factor 1 signaling pathways, which have been previously associated with AML growth and development. Furthermore, programmed death-1 ligand 1 was reported to facilitate AML progression through the PI3K/AKT signaling pathway (32). These results underscore the importance of exploring the ARS model importance in AML.

The present study analyzed the TCGA and GSE71014 cohorts, revealing that LGALS1, ITGA4, HGF and RHOC were significantly associated with AML prognosis. Meanwhile, ITGA4 and HGF were positively associated with AML, whilst LGALS1 and RHOC demonstrated a negative association with it, consistent with previous studies (10,11,34). Future research should involve larger sample sizes and cellular-level experiments to clarify the specific roles of each prognostic gene in AML.

Conventional induction chemotherapy has traditionally been the frontline therapy for AML. However, therapy resistance remains a challenge, necessitating the development of new chemotherapeutic drugs. Dasatinib was reported to induce c-KIT-positive AML cell death via caspase-dependent apoptosis (45), BI 2536 was reported to induce mitotic arrest and apoptosis in AML cells (46), and taxol was reported to suppress microtubule dynamics, inducing mitotic arrest, triggering caspase-3 cleavage and inducing apoptosis in human AML HL-60 cells (47). Furthermore, lapatinib was reported to effectively suppress the proliferation of AML cell lines in a dose- and time-dependent manner, inducing either autophagic or apoptotic cell death (48). PD0325901 also effectively blocks MEK/ERK signaling, with strong inhibitory and apoptotic effects, especially in AML (49), Jw-7-52-1 was effective in treating AML (50), and erlotinib was reported to target Fms-related tyrosine kinase 3 and Lyn, overcoming intratumoral heterogeneity in AML (51). Moreover, the interruption of the canonical NF-κB pathway may enhance the lethality of belinostat when combined with bortezomib in AML cells (52). Roscovitine, combined with all-trans retinoic acid, was reported to induce nuclear enrichment of proteins promoting differentiation and cell cycle arrest in t(15;17)-negative HL-60 human myeloblastic leukemia cells (53). The dual insulin-like growth factor 1 receptor/insulin receptor, inhibitor BMS-536924 was also

reported to reduce autophosphorylation of its target receptors through the PI3K/AKT and MAPK pathways and inhibit proliferation and colony formation in AML cell lines and clinical AML samples (54).

Although the proposed ARS model in the present study demonstrates promising predictive power for AML prognosis, the present study has certain limitations. First, all clinical AML cohorts analyzed were sourced solely from TCGA website, necessitating validation of the ARS model using external cohorts. Second, the expression patterns of the ARS genes need to be confirmed in clinical specimens using molecular biology techniques, and further research is required to elucidate the underlying mechanisms of ARS genes through experimental analyses.

In summary, the present study developed a novel gene signature related to anoikis in AML. The inclusion of ARS genes significantly enhances the prediction of AML survival outcomes and effectively stratifies the risk among patients with AML. The present study offers a fresh perspective on therapeutic strategies for individuals with AML.

Availability of data and materials

The TCGA datasets used in the present study can be accessed at https://www.cancer.gov/about-nci/organization/ccg/research/structural-genomics/tcga, whilst the GEO datasets are available at https://www.ncbi.nlm.nih.gov/geo/ as dataset GSE71014. The data generated in the present study are included in the supplementary figures and/or tables of this article.

Authors' contributions

YDC, YH and JSW conceived the study, wrote the manuscript and revised it. YDC, WCL and MYH performed the experiments and contributed to data analysis. WCL and XYY collected clinical sample data. JSW also revised the manuscript. All authors have read and approved the final manuscript, agreed to be accountable for all aspects of the work and contributed to data analysis as well as drafting or revising the article. YDC and YH confirm the authenticity of all the raw data.

Ethics approval and consent to participate

Prior to performing the present study, ethical approval was obtained from The Ethics Committee of the Affiliated Hospital of Guizhou Medical University (Guiyang, China; approval no. 2023-744). The participants were informed about the purpose of the research, the assurance of anonymity and the storage procedures for their collected data. Informed consent was obtained from all participants before commencing with the

study and all participants consented to the disclosure of their medical data.

Patient consent for publication

Not applicable.

Competing interests

The authors declare that they have no competing interests.

References

1. Izadirad M, Jafari L, James AR, Unfried JP, Wu ZX and Chen ZS: Long noncoding RNAs have pivotal roles in chemoresistance of acute myeloid leukemia. Drug Discov Today 26: 1735-1743, 2021.
2. SEER. Cancer Stat Facts: Leukemia-Acute Myeloid Leukemia (AML). 2023. Available from: https://seer.cancer.gov/statfacts/html/amyl.html.
3. Riva L, Luzi L and Pelicci PG: Genomics of acute myeloid leukemia: The next generation. Front Oncol 2: 40, 2012.
4. Han HJ, Sung JY, Kim SH, Yun UJ, Kim H, Jang EJ, Yoo HE, Hong EK, Goh SH, Moon A, et al: Fibronectin regulates anoikis resistance via cell aggregate formation. Cancer Lett 508: 59-72, 2021.
5. Adeshakin FO, Adeshakin AO, Afolabi LO, Yan D, Zhang G and Wan X: Mechanisms for modulating anoikis resistance in cancer and the relevance of metabolic reprogramming. Front Oncol 11: 626577, 2021.
6. Ye G, Yang Q, Lei X, Zhu X, Li F, He J, Chen H, Ling R, Zhang H, Lin T, et al: Nuclear MYH9-induced CTNNB1 transcription, targeted by staurosporin, promotes gastric cancer cell anoikis resistance and metastasis. Theranostics 10: 7545-7560, 2020.
7. Jin L, Chun J, Pan C, Kumar A, Zhang G, Ha Y, Li D, Alesi GN, Kang Y, Zhou L, et al: The PLAG1-GDH1 axis promotes anoikis resistance and tumor metastasis through CamKK2-AMPK signaling in LKB1-Deficient lung cancer. Mol Cell 69: 87-99.e7, 2018.
8. Buchheit CL, Angarola BL, Steiner A, Weigel KJ and Schafer ZT: Anoikis evasion in inflammatory breast cancer cells is mediated by Bim-EL sequestration. Cell Death Differ 22: 1275-1286, 2015.
9. Chen J, Gao F and Liu N: L1CAM promotes epithelial to mesenchymal transition and formation of cancer initiating cells in human endometrial cancer. Exp Ther Med 15: 2792-2797, 2018.
10. Ruvolo PP, Ma H, Ruvolo VR, Zhang X, Post SM and Andreeff M: LGALS1 acts as a pro-survival molecule in AML. Biochim Biophys Acta Mol Cell Res 1867: 118785, 2020.
11. Nie D, Ma P, Chen Y, Zhao H, Liu L, Xin D, Cao W, Wang F, Meng X, Liu L, et al: MiR-204 suppresses the progression of acute myeloid leukemia through HGF/c-Met pathway. Hematology 26: 931-939, 2021.
12. Zhang J, Qi L, Wang T, An J, Zhou B, Fang Y, Liu Y, Shan M, Hong D, Wu D, et al: FEV maintains homing and expansion by activating ITGA4 transcription in primary and relapsed AML. Front Oncol 12: 890346, 2022.
13. Lou Y, Jiang Y, Liang Z, Liu B, Li T and Zhang D: Role of RhoC in cancer cell migration. Cancer Cell Int 21: 527, 2021.
14. Chen S, Gu J, Zhang Q, Hu Y and Ge Y: Development of biomarker signatures associated with anoikis to predict prognosis in endometrial carcinoma patients. J Oncol 2021: 3375297, 2021.
15. Yu G, Wang LG, Han Y and He QY: clusterProfiler: An R package for comparing biological themes among gene clusters. OMICS 16: 284-287, 2012.
16. Ritchie ME, Phipson B, Wu D, Hu Y, Law CW, Shi W and Smyth GK: Limma powers differential expression analyses for RNA-sequencing and microarray studies. Nucleic Acids Res 43: e47, 2015.
17. Wu X, Sui Z, Zhang H, Wang Y and Yu Z: Integrated analysis of lncRNA-mediated ceRNA network in lung adenocarcinoma. Front Oncol 10: 554759, 2020.
18. Friedman J, Hastie T and Tibshirani R: Regularization paths for generalized linear models via coordinate descent. J Stat Softw 33: 1-22, 2010.
19. Liu TT, Li R, Huo C, Li JP, Yao J, Ji XL and Qu YQ: Identification of CDK2-related immune forecast model and ceRNA in lung adenocarcinoma, a Pan-cancer analysis. Front Cell Dev Biol 9: 682002, 2021.
20. Heagerty PJ, Lumley T and Pepe MS: Time-dependent ROC curves for censored survival data and a diagnostic marker. Biometrics 56: 337-344, 2000.
21. Xu J, Yang T, Wu F, Chen T, Wang A and Hou S: A nomogram for predicting prognosis of patients with cervical cerclage. Heliyon 9: e21147, 2023.
22. De Kouchkovsky I and Abdul-Hay M: 'Acute myeloid leukemia: A comprehensive review and 2016 update'. Blood Cancer J 6: e441, 2016.
23. Gu Z, Eils R and Schlesner M: Complex heatmaps reveal patterns and correlations in multidimensional genomic data. Bioinformatics 32: 2847-2849, 2016.
24. Livak KJ and Schmittgen TD: Analysis of relative gene expression data using real-time quantitative PCR and the 2(-Delta Delta C(T)) method. Methods 25: 402-408, 2001.
25. Maeser D, Gruener RF and Huang RS: oncoPredict: An R package for predicting in vivo or cancer patient drug response and biomarkers from cell line screening data. Brief Bioinform 22: bbab260, 2021.
26. Döhner H, Estey E, Grimwade D, Amadori S, Appelbaum FR, Büchner T, Dombret H, Ebert BL, Fenaux P, Larson RA, et al: Diagnosis and management of AML in adults: 2017 ELN recommendations from an international expert panel. Blood 129: 424-447, 2017.
27. Almond LM, Charalampakis M, Ford SJ, Gourevitch D and Desai A: Myeloid SArcoma: Presentation, diagnosis, and treatment. Clin Lymphoma Myeloma Leuk 17: 263-267, 2017.
28. Bakir B, Chiarella AM, Pitarresi JR and Rustgi AK: EMT, MET, plasticity, and tumor metastasis. Trends Cell Biol 30: 764-776, 2020.
29. Jin L, Chun J, Pan C, Alesi GN, Li D, Magliocca KR, Kang Y, Chen ZG, Shin DM, Khuri FR, et al: Phosphorylation-mediated activation of LDHA promotes cancer cell invasion and tumour metastasis. Oncogene 36: 3797-3806, 2017.
30. Jiang K, Yao G, Hu L, Yan Y, Liu J, Shi J, Chang Y, Zhang Y, Liang D, Shen D, et al: MOB2 suppresses GBM cell migration and invasion via regulation of FAK/Akt and cAMP/PKA signaling. Cell Death Dis 11: 230, 2020.
31. Kim H, Choi P, Kim T, Kim Y, Song BG, Park YT, Choi SJ, Yoon CH, Lim WC, Ko H and Ham J: Ginsenosides Rk1 and Rg5 inhibit transforming growth factor-β1-induced epithelial-mesenchymal transition and suppress migration, invasion, anoikis resistance, and development of stem-like features in lung cancer. J Ginseng Res 45: 134-148, 2021.
32. Wang F, Yang L, Xiao M, Zhang Z, Shen J, Anuchapreeda S, Tima S, Chiampanichayakul S and Xiao Z: PD-L1 regulates cell proliferation and apoptosis in acute myeloid leukemia by activating PI3K-AKT signaling pathway. Sci Rep 12: 11444, 2022.
33. Kamili NA, Arthur CM, Gerner-Smidt C, Tafesse E, Blenda A, Dias-Baruffi M and Stowell SR: Key regulators of galectin-glycan interactions. Proteomics 16: 3111-3125, 2016.
34. Li M, Ye J, Xia Y, Li M, Li G, Hu X, Su X, Wang D, Zhao X, Lu F, et al: METTL3 mediates chemoresistance by enhancing AML homing and engraftment via ITGA4. Leukemia 36: 2586-2595, 2022.
35. Wang SH, Wu XC, Zhang MD, Weng MZ, Zhou D and Quan ZW: Upregulation of H19 indicates a poor prognosis in gallbladder carcinoma and promotes epithelial-mesenchymal transition. Am J Cancer Res 6: 15-26, 2016.
36. Chen EC, Gandler H, Tošić I, Fell GG, Fiore A, Pozdnyakova O, DeAngelo DJ, Galinsky I, Luskin MR, Wadleigh M, et al: Targeting MET and FGFR in relapsed or refractory acute myeloid leukemia: Preclinical and clinical findings, and signal transduction correlates. Clin Cancer Res 29: 878-887, 2023.
37. Guo JR, Li W, Wu Y, Wu LQ, Li X, Guo YF, Zheng XH, Lian XL, Huang HF and Chen YZ: Hepatocyte growth factor promotes proliferation, invasion, and metastasis of myeloid leukemia cells through PI3K-AKT and MAPK/ERK signaling pathway. Am J Transl Res 8: 3630-3644, 2016.
38. Lawson CD and Ridley AJ: Rho GTPase signaling complexes in cell migration and invasion. J Cell Biol 217: 447-457, 2018.
39. Stanley A, Thompson K, Hynes A, Brakebusch C and Quondamatteo F: NADPH oxidase complex-derived reactive oxygen species, the actin cytoskeleton, and Rho GTPases in cell migration. Antioxid Redox Signal 20: 2026-2042, 2014.

40. Liu BL, Sun KX, Zong ZH, Chen S and Zhao Y: MicroRNA-372 inhibits endometrial carcinoma development by targeting the expression of the Ras homolog gene family member C (RhoC). Oncotarget 7: 6649-6664, 2016.
41. Knirsh R, Ben-Dror I, Modai S, Shomron N and Vardimon L: MicroRNA 10b promotes abnormal expression of the proto-onco-gene c-Jun in metastatic breast cancer cells. Oncotarget 7: 59932-59944, 2016.
42. Wang YF, Li Z, Zhao XH, Zuo XM, Zhang Y, Xiao YH, Li J and Peng ZH: MicroRNA-10b is upregulated and has an invasive role in colorectal cancer through enhanced Rhoc expression. Oncol Rep 33: 1275-1283, 2015.
43. Sang XB, Zong ZH, Wang LL, Wu DD, Chen S, Liu BL and Zhao Y: E2F-1 targets miR-519d to regulate the expression of the ras homolog gene family member C. Oncotarget 8: 14777-14793, 2017.
44. Zhou W, Zhang C, Jiang H, Zhang Z, Xie L and He X: MiR-493 suppresses the proliferation and invasion of gastric cancer cells by targeting RhoC. Iran J Basic Med Sci 18: 1027-1033, 2015.
45. Heo SK, Noh EK, Kim JY, Jeong YK, Jo JC, Choi Y, Koh S, Baek JH, Min YJ and Kim H: Targeting c-KIT (CD117) by dasat-inib and radotinib promotes acute myeloid leukemia cell death. Sci Rep 7: 15278, 2017.
46. Müller-Tidow C, Bug G, Lübbert M, Krämer A, Krauter J, Valent P, Nachbaur D, Berdel WE, Ottmann OG, Fritsch H, *et al*: A randomized, open-label, phase I/II trial to investigate the maximum tolerated dose of the Polo-like kinase inhibitor BI 2536 in elderly patients with refractory/relapsed acute myeloid leukaemia. Br J Haematol 163: 214-222, 2013.
47. Ibrado AM, Kim CN and Bhalla K: Temporal relationship of CDK1 activation and mitotic arrest to cytosolic accumulation of cytochrome C and caspase-3 activity during Taxol-induced apoptosis of human AML HL-60 cells. Leukemia 12: 1930-1936, 1998.
48. Chen YJ, Fang LW, Su WC, Hsu WY, Yang KC and Huang HL: Lapatinib induces autophagic cell death and differentiation in acute myeloblastic leukemia. Onco Targets Ther 9: 4453-4464, 2016.
49. Ricciardi MR, Scerpa MC, Bergamo P, Ciuffreda L, Petrucci MT, Chiaretti S, Tavolaro S, Mascolo MG, Abrams SL, Steelman LS, *et al*: Therapeutic potential of MEK inhibition in acute myelogenous leukemia: Rationale for 'vertical' and 'lateral' combination strategies. J Mol Med (Berl) 90: 1133-1144, 2012.
50. Wang Z, Liu Y, Mo Y, Zhang H, Dai Z, Zhang X, Ye W, Cao H, Liu Z and Cheng Q: The CXCL family contributes to immuno-suppressive microenvironment in gliomas and assists in gliomas chemotherapy. Front Immunol 12: 731751, 2021.
51. Cao ZX, Guo CJ, Song X, He JL, Tan L, Yu S, Zhang RQ, Peng F, Peng C and Li YZ: Erlotinib is effective against FLT3-ITD mutant AML and helps to overcome intratumoral heterogeneity via targeting FLT3 and Lyn. FASEB J 34: 10182-10190, 2020.
52. Dai Y, Chen S, Wang L, Pei XY, Kramer LB, Dent P and Grant S: Bortezomib interacts synergistically with belinostat in human acute myeloid leukaemia and acute lymphoblastic leukaemia cells in association with perturbations in NF-κB and Bim. Br J Haematol 153: 222-235, 2011.
53. Rashid A, Duan X, Gao F, Yang M and Yen A: Roscovitine enhances all-trans retinoic acid (ATRA)-induced nuclear enrichment of an ensemble of activated signaling molecules and augments ATRA-induced myeloid cell differentiation. Oncotarget 11: 1017-1036, 2020.
54. Wahner Hendrickson AE, Haluska P, Schneider PA, Loegering DA, Peterson KL, Attar R, Smith BD, Erlichman C, Gottardis M, Karp JE, *et al*: Expression of insulin receptor isoform A and insulin-like growth factor-1 receptor in human acute myelogenous leukemia: Effect of the dual-receptor inhibitor BMS-536924 in vitro. Cancer Res 69: 7635-7643, 2009.